The Human Arm Kinematics and Dynamics During Daily Activities – Toward a 7 DOF Upper Limb Powered Exoskeleton

Jacob Rosen [1], Joel C. Perry [2], Nathan Manning [1], Stephen Burns [3], Blake Hannaford [1]
[1] *Department of Electrical Engineering Box 352500*
[2] *Department of Mechanical Engineering Box 358725*
[3] *Department of Rehabilitation Medicine Box 356490*
University of Washington, Seattle WA, 98185, USA

E:mail: <rosen, jcperry, spburns, blake>@u.washington.edu; URL: http://brl.ee.washington.edu

***Abstract*— Integrating human and robot into a single system offers remarkable opportunities for creating a new generation of assistive technology. Having obvious applications in rehabilitation medicine and virtual reality simulation, such a device would benefit both the healthy and disabled population. The aim of the research is to study the kinematics and the dynamics of the human arm during daily activities in a free and unconstrained environment as part of an on-going research involved in the design of a 7 degree of freedom (DOF) powered exoskeleton for the upper limb. The kinematics of the upper limb was acquired with a motion capture system while performing a wide verity of daily activities. Utilizing a model of the human as a 7 DOF system, the equations of motion were used to calculate joint torques given the arm kinematics. During positioning tasks, higher angular velocities were observed in the gross manipulation joints (the shoulder and elbow) as compared to the fine manipulation joints (the wrist). An inverted phenomenon was observed during fine manipulation in which the angular velocities of the wrist joint exceeded the angular velocities of the shoulder and elbow joints. Analyzing the contribution of individual terms of the arm's equations of motion indicate that the gravitational term is the most dominant term in these equations. The magnitudes of this term across the joints and the various actions is higher than the inertial, centrifugal, and Coriolis terms combined. Variation in object grasping (e.g. power grasp of a spoon) alters the overall arm kinematics in which other joints, such as the shoulder joint, compensate for lost dexterity of the wrist. The collected database along with the kinematics and dynamic analysis may provide the fundamental understanding for designing powered exoskeleton for the human arm.**

***Index Terms*— Daily Activities, Exoskeleton, Human Arm, Orthotics, Wearable Robotics.**

I. INTRODUCTION

Integrating human and robot into a single system offers remarkable opportunities for creating a new generation of assistive technology for both healthy and disabled people. Humans possess naturally developed algorithms for control of movement, but are limited by their muscle strength. Additionally, for most people with neuromuscular diseases (NMD) and central nervous system injuries, muscle weakness is the primary cause of disability. In contrast, robotic manipulators can perform tasks requiring large forces; however, their artificial control algorithms do not provide the flexibility to perform in a wide range of fuzzy conditions while preserving the same quality of performance as humans. It seems therefore that combining these two entities, the human and the robot, into one integrated system under the control of the human, may lead to a solution that will benefit from the advantages offered by each subsystem.

The exoskeleton robot, serving as an assistive device, is worn by the human (orthotic) and functions as a human-amplifier. Its joints and links correspond to those of the human body, and its actuators share a portion of the external load with the operator.

A wide variety of exoskeleton systems both for upper and lower limbs with various human machine interfaces have been developed (for review see [1]). The design of an exoskeleton as a wearable device should rely not just on anthropometric information of the human body [2],[3] but also on comprehensive information regarding human body kinematics and dynamics. Previous research regarding the human upper limb focused mainly on arm kinematics [4]. In addition to the human arm kinematics, the current study is centered around arm dynamics. The study is part of an on-going research effort toward the development of a 7 degree of freedom powered exoskeleton for the human arm (Fig. 1).

This work is supported by NSF Grant #0208468 entitled "Neural Control of an Upper Limb Exoskeleton System" - Jacob Rosen (PI)

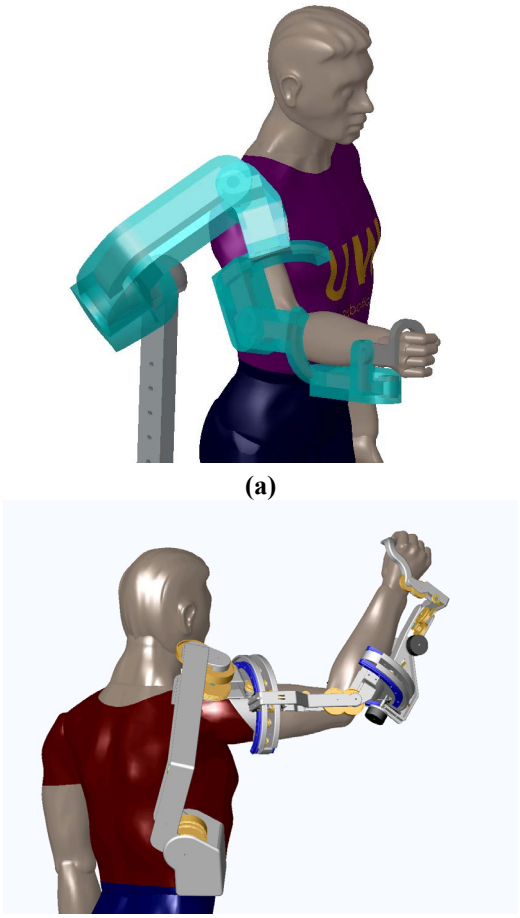

Fig. 1: An Exoskeleton arm: **(a)** CAD rendering of 7 degree of freedom (DOF) upper limb powered exoskeleton (shoulder joint - 3 DOF, elbow joint – 1 DOF, wrist joint 3 DOF **(b)** An exposed view of the Exoskeleton arm in a reach posture.

II. Methods and Tools

A. Kinematics – Experimental Protocol

The kinematic data of the human arm of a single subject during daily activities were collected using the VICON motion capture system (Vicon Inc.) at a sampling frequency of 120 Hz. Reflective markers were attached to a subject at key anatomical locations (Figure 2a). The subject was instructed to perform three repetitions of the same arm activity. The arm activities were divided into two subgroups: (1) general motions, and (2) actions (daily activities). Selecting the specific human arm actions was based on previous surveys of the disabled community indicating the desired tasks and functionality of powered orthotic devices and rehabilitation robots [5],[6]. The general motion included a movement through a full range of motion of each of the human arm joints in a standing posture. The human arm actions during daily activities were performed in either standing or sitting body posture depending on the nature of the activity. During these activities the subject interacted with various small objects as dictated by each activity in an unconstrained environment. All motions and activities were performed using the subjects' right (dominate) arm. Given these conditions, no external forces or torques were applied on the human. Every action and general motion started from an initial arm position in which the arm was fully extended along the body. The following arm activities were included in the experimental protocol:

General Motion

1. Elbow flexion/extension
2. Elbow rotation (supination/pronation)
3. Shoulder adduction/abduction
4. Shoulder flexion/extension
5. Shoulder interior/exterior rotation
6. Wrist flexion/extension
7. Wrist ulnar/radial deviation
8. Shoulder horizontal flexion/extension
9. Full-range shoulder free motion

Actions

1. Arm in lap
2. Arm reach to head level
3. Arm reach to right, head level
4. Arm reach to left, head level
5. Arm reach right, move object to left side
6. Open door
7. Open Drawer/Close Drawer
8. Move object at waist level
9. Pick up phone on table/hang up
10. Pick up phone on wall/hang up
11. Eat with fork
12. Eat with spoon
13. Eat with hands
14. Drink with cup
15. Eat with spoon
16. Pour from bottle
17. Brush teeth
18. Comb hair
19. Wash face
20. Wash neck
21. Shave
22. Eat with fork (power – disabled grasp)
23. Eat with spoon (power – disabled grasp)
24. Full workspace motion

The arm action associated with eating with a spoon and a fork had two variations. Actions 11 and 12 involved normal fork/spoon handling where the fingers were used to orient the fork and spoon. In actions 22 and 23, a power gasp of the fork/spoon along with maximal wrist joint flexion was used to emulate a method of fork/spoon handling commonly exhibited by patients who suffer from one of several neurological disorders.

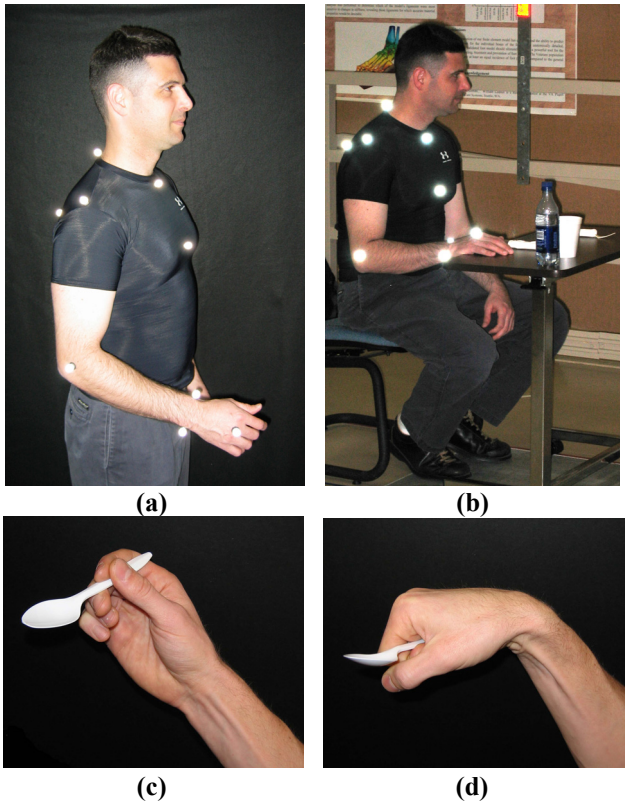

Fig. 2: Experimental Setup: **(a)** Reflective markers of a motion capture system attached to a subject at key anatomical locations **(b)** Motion capture of a subject's upper arm kinematics interacting with objects in daily activities **(c)** Holding a spoon with normal hand grasp **(d)** holding a spoon using a power grasp along with full wrist joint flexion, a typical pathology developed among several neurological disorders.

For each arm motion, Euler joint angles for the seven degrees of freedom (DOF) of the human arm were calculated based on the Cartesian coordinates of each marker. This transformation was performed based on an inherent model of the body that is incorporated into the Vicon system. The model incorporates anthropometric data that was measured directly from the subject under study. Each action was videotaped synchronously with the data collection performed by the Vicon system. A simulation of collected data using the human model within the Vicon system was compared with the video clip to ensure the appropriate transformation between marker coordinates and the calculated joint angles.

B. Dynamics – Post Processing

The human arm dynamics were studied using analytical and numerical approaches. A model of the human arm with 7 DOF was developed. Analytical expressions of the seven equations of motion were developed using Autolev (OnLine Dynamics Inc.). In addition, the dynamics of the human arm was simulated numerically using a numerical model within COSMOS/Motion, powered by the ADAMS® simulation engine. COSMOS/Motion is a virtual prototyping package for use with Solidworks CAD software. The coordinate systems that were assigned to each link of the human arm are depicted in Fig. 3.

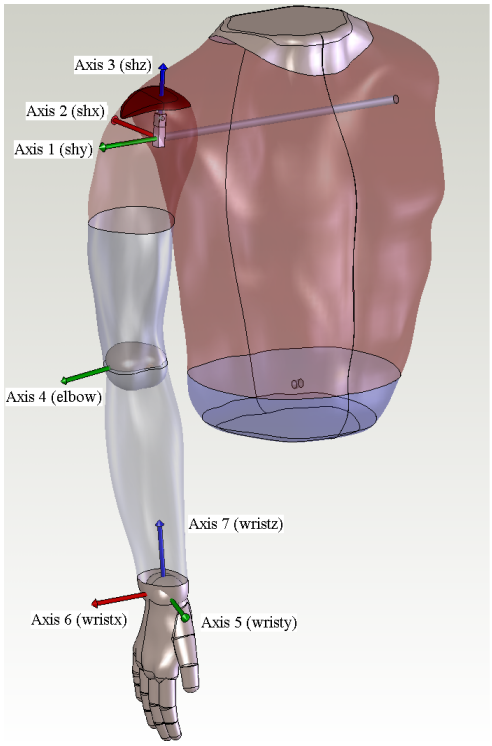

Fig. 3: The human arm model and coordinate system assignments for each link of the human arm. Arm and torso model from BodyWorks (Zetec Ltd.).

The general form of the equations of motion is expressed in Eq. 1.

$$\tau = M(\Theta)\ddot{\Theta} + V(\Theta, \dot{\Theta}) + G(\Theta) \qquad (1)$$

where $M(\Theta)$ is the 7x7 mass matrix, $V(\Theta, \dot{\Theta})$ is a 7x1 vector of centrifugal and Coriolis terms, $G(\Theta)$ is a 7x1 vector of gravity terms, and τ is a 7x1 vector of the net toques applied at the joints. Given the kinematics of the human arm ($\ddot{\Theta}, \dot{\Theta}, \Theta$) the net joints toque ($\tau$) vector was calculated with and without the gravitational effect. These two parallel calculations allow one to examine the contribution of gravity in comparison to the combined effects on net torque from inertial, centrifugal, and Coriolis forces. In this case, the contributions from gravity could not be computed directly due to the size and complexity of involved equations.

III. Results

Figure 4a depicts typical time histories of the seven rotation angles, angular velocities, angular accelerations, and joint axes torques associated with one repetition of action 2 - Arm reach to the head level. In Figure 4b, the statistical distribution of the same information depicted in Fig. 4a is plotted. Similar statistical distributions for two other actions are plotted in Figure 5, including (1) moving an object at the waist level – action 8, and (2) picking up a phone on a wall – action 10.

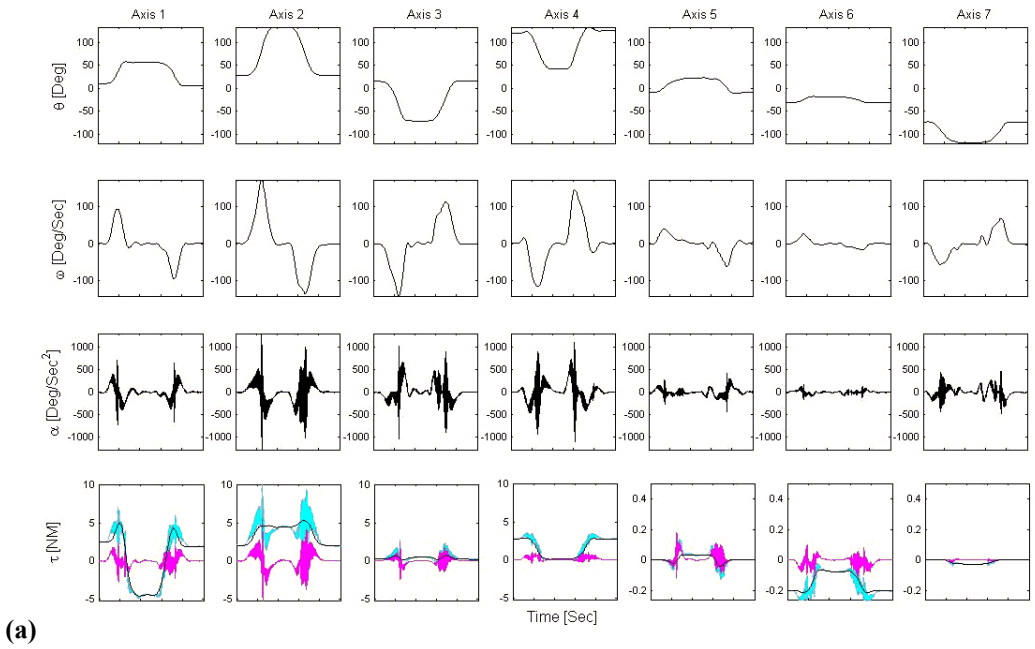

(a)

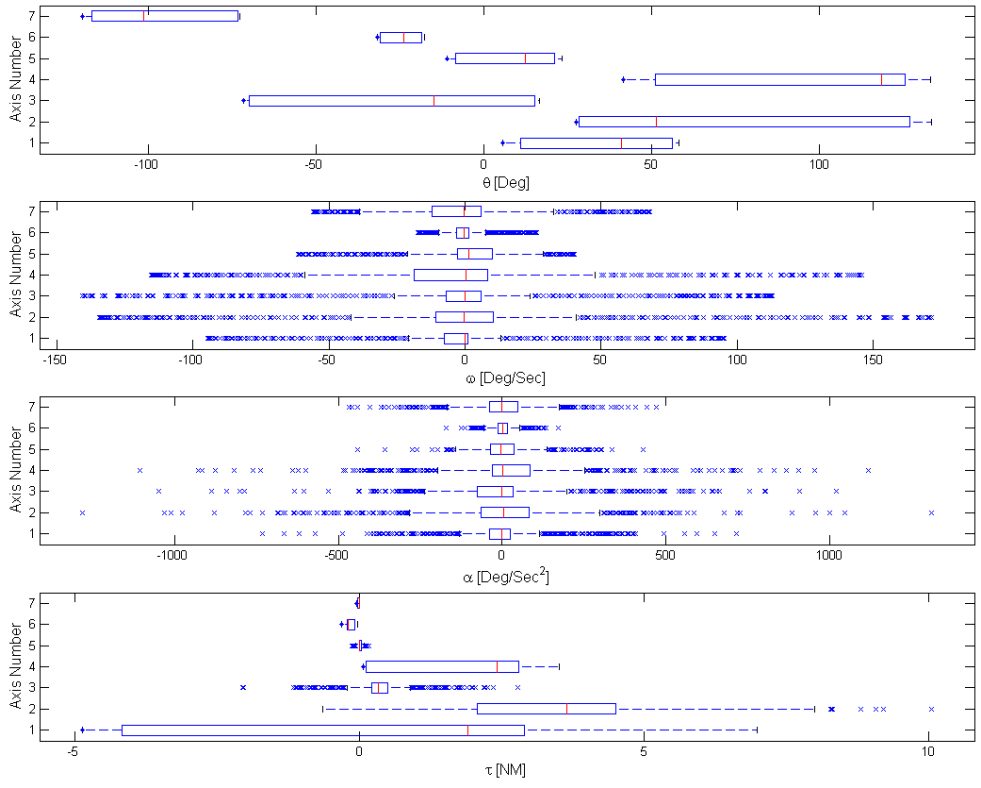

(b)

Fig. 4: Time histories and statistics of the kinematics and dynamics of the human arm during an arm reach to head level (action 2): **(a)** Time histories of the joint kinematics and dynamics **(b)** Statistical distribution of the joint kinematics and dynamics. The three torque curves in (a) illustrate the total joint axis torque (cyan), in comparison to the gravitational torque (black) and the combined torque due to inertial, centrifugal, and coriolis terms (magenta). The line box plots of (b) indicate the lower quartile, median, and upper quartile values. The dashed lines extend beyond the upper and lower quartiles by one and a half times the interquartile range. Data that lies outside of this range is displayed with the symbol 'x'.

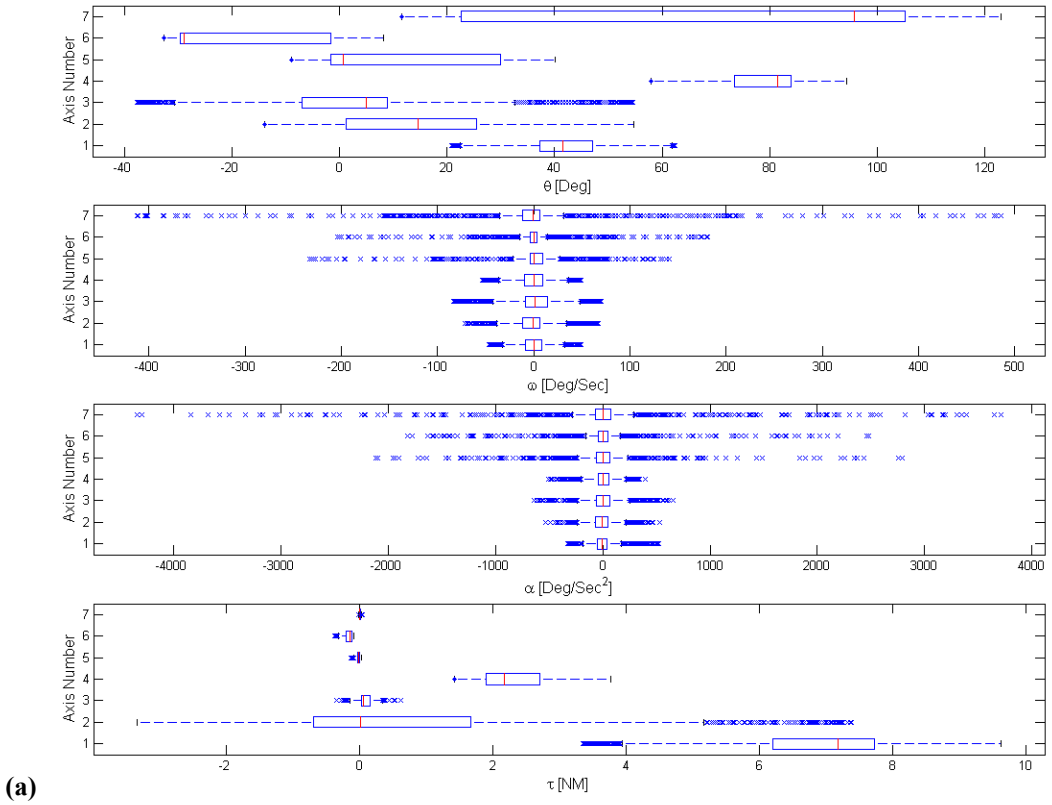

(a)

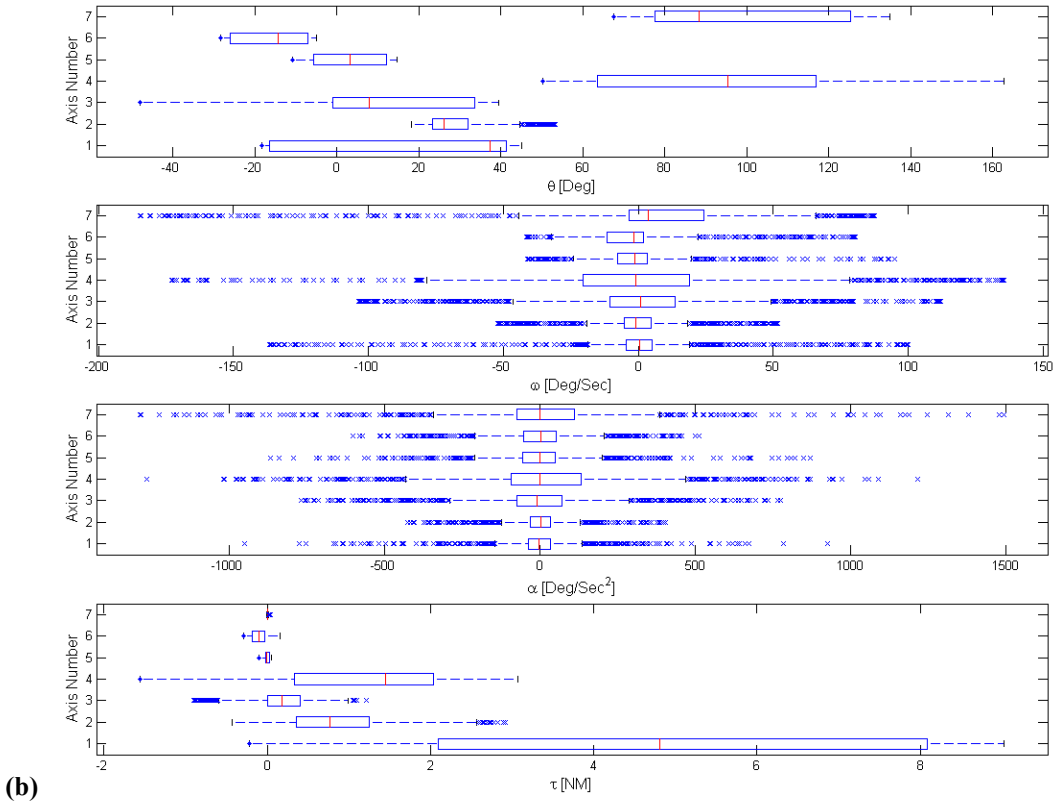

(b)

Fig. 5: Statistics of the kinematics and dynamics of the human arm during various upper arm daily activities: **(a)** Statistical distribution of the joint kinematics and dynamics while moving an object at waist level (action 8), and **(b)** Statistical distribution of the joint kinematics and dynamics while picking and then hanging up a wall-mounted phone (action 10). See figure 4 caption for explanation of box plot features.

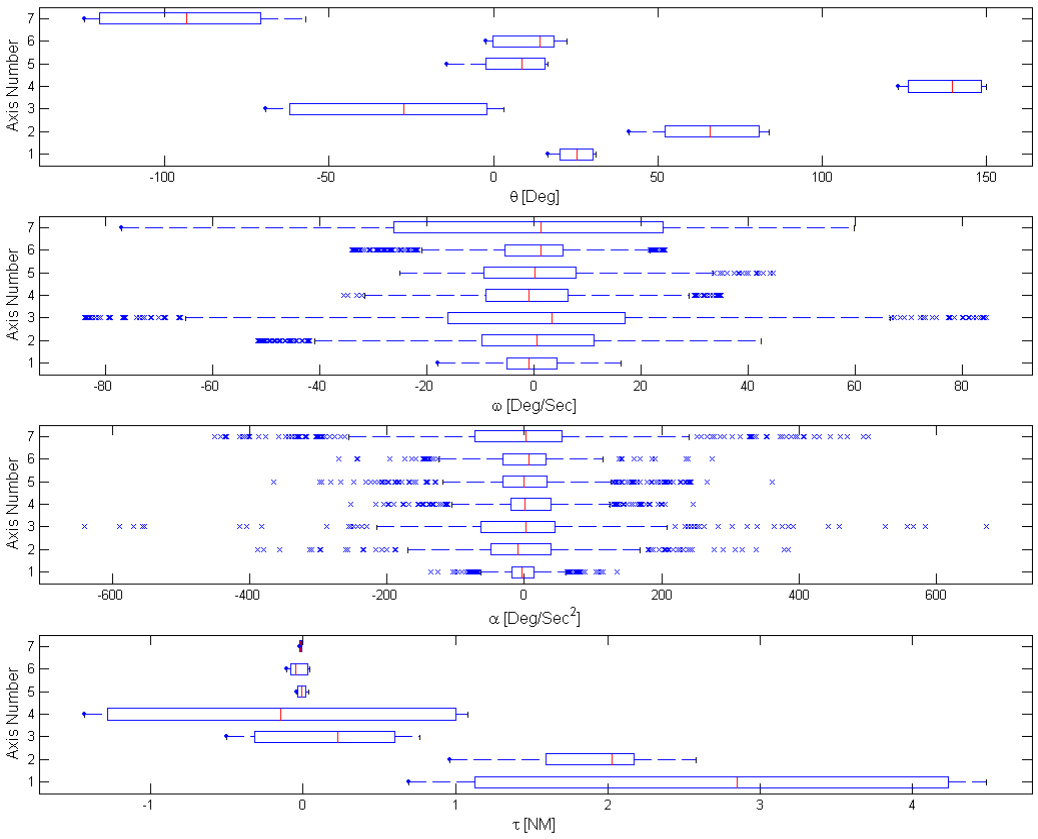

(a)

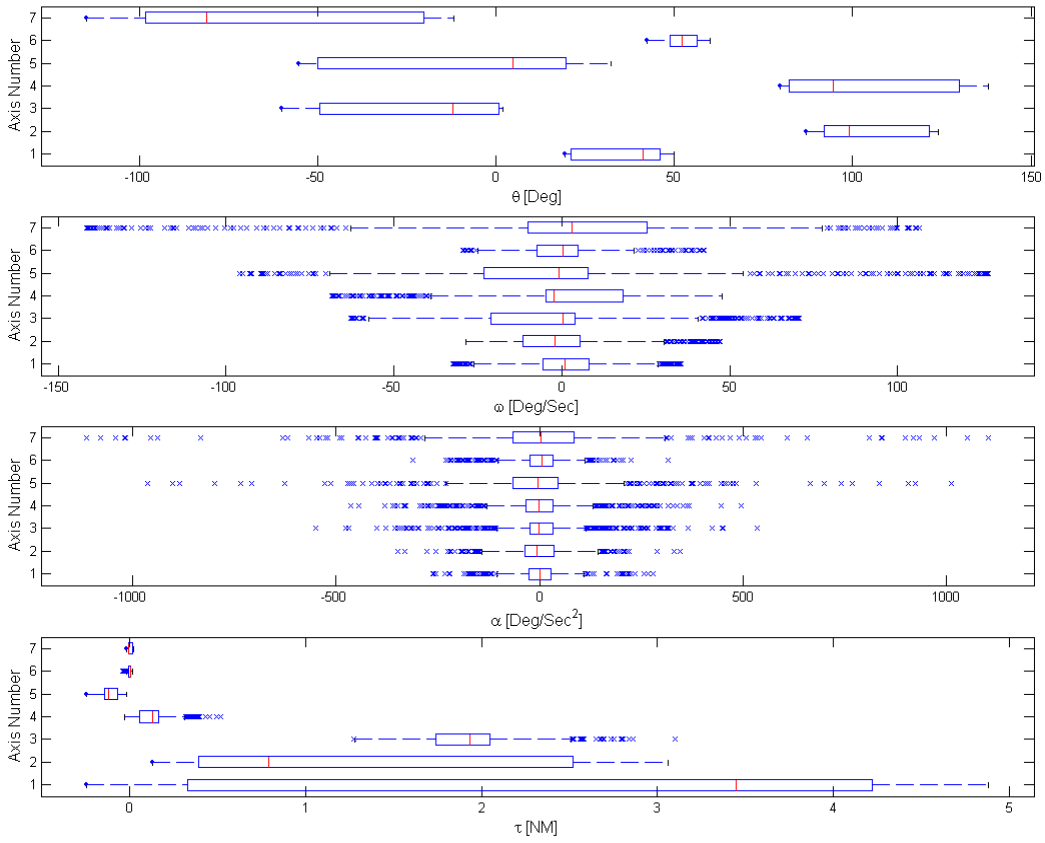

(b)

Fig. 6: The human arm kinematics and dynamics statistical distribution while eating with a spoon using **(a)** normal spoon grasp – action 12, and **(b)** power spoon grasp, a typical pathology developed among several neurological disorders – action 23. See figure 4 caption for explanation of box plot features.

Table I: Summary of all the kinematic and dynamic ranges along with mean and median values for actions 2, 8, 10, 12, and 23. Data includes min, max, mean, and median values for angles (deg), angular velocities (deg/s), angular accelerations (deg/s^2), and torques (Nm) at each joint. Two torque values are provided, the total joint torque (torTot) and the velocity/acceleration-dependent torque (torAV), i.e., the torque required to position the arm without the presence of gravity. For correlation between joint label and corresponding axis label (for example shy = axis 1), see Fig 3.

		shy				shx				shz				elbow				wristy				wristx				wristz			
		min	max	mean	median	min	max	mean	median	min	max	mean	median	min	max	mean	median	min	max	mean	median	min	max	mean	median	min	max	mean	median
act02	theta	5.7	58.2	33.9	41.0	27.5	133.6	71.7	51.5	-71.7	16.7	-23.9	-14.8	41.7	133.1	94.6	118.6	-23.3	11.0	-8.0	-12.4	17.6	31.7	24.7	24.0	-119.8	-72.8	-97.2	-101.5
	vel	-94.6	95.0	-0.9	-0.1	-134.1	171.5	0.0	-0.2	-140.7	113.0	0.2	-0.1	-115.4	145.8	1.3	0.5	-40.2	61.1	0.0	-1.4	-26.5	17.3	0.0	0.2	-55.8	67.9	-0.1	-0.5
	accel	-732.7	715.4	2.6	-0.4	-1282.7	1311.7	-1.7	4.5	-1049.0	1020.3	3.2	-1.2	-1104.7	1117.5	6.0	2.2	-429.5	441.8	-3.6	5.0	-171.9	171.6	-1.1	-0.4	-466.9	471.2	-2.5	-1.0
	torTot	-4869.4	6990.1	297.8	1904.1	-640.4	10057.0	3609.1	3650.0	-2040.8	2791.2	368.8	341.2	73.2	3513.6	1704.1	2413.0	-173.0	128.6	-12.1	0.0	21.8	307.1	157.1	197.7	-40.6	3.2	-9.9	-1.7
	torAV	-2854.9	2276.5	5.3	-5.1	-5210.1	5492.0	53.1	19.0	-2416.6	2426.4	14.8	1.7	-516.5	1050.1	129.3	1.7	-179.1	118.3	-6.8	0.0	-100.4	119.9	8.7	0.2	-20.9	6.7	-0.3	-0.1
act08	theta	20.8	62.3	42.3	41.6	-14.0	54.6	16.7	14.6	-37.8	54.6	5.3	4.9	58.0	94.4	78.3	81.5	-40.1	9.1	-10.8	-0.6	-8.1	32.7	19.6	29.0	11.5	123.2	74.7	95.7
	vel	-46.9	48.9	0.1	0.0	-71.9	67.2	0.2	-0.8	-83.7	70.0	-0.5	1.5	-53.2	49.6	0.4	0.3	-141.2	232.9	-0.4	-0.4	-180.4	203.9	-0.3	-0.2	-412.8	486.3	-0.4	-0.3
	accel	-330.5	517.1	-0.4	-3.2	-534.7	531.7	-1.4	-8.6	-640.3	657.3	6.3	1.3	-507.7	398.6	-4.0	1.3	-2790.1	2116.2	-1.1	-2.5	-2476.2	1822.4	-0.1	0.5	-4343.6	3715.5	-1.6	2.5
	torTot	3344.7	9626.0	6841.9	7169.9	-3344.3	7377.1	947.9	17.9	-348.5	610.4	95.6	61.7	1417.4	3763.1	2271.1	2171.1	-21.9	132.4	23.2	11.6	83.2	373.8	160.2	147.9	-21.7	43.5	2.8	-0.1
	torAV	-1694.0	3245.1	-16.1	-17.9	-2344.5	2504.7	1.5	-7.4	-582.9	437.8	-18.9	-0.8	-610.2	1081.3	13.5	15.6	-43.0	42.8	-1.2	-0.3	-80.6	169.6	-0.3	0.8	-8.7	11.7	0.0	0.0
act10	theta	-18.3	45.0	20.1	37.3	18.2	53.2	29.2	26.2	-48.1	39.5	6.0	8.0	50.3	162.9	99.0	95.3	-14.6	10.8	-3.0	-3.3	5.1	28.3	15.7	14.4	67.6	134.9	98.1	88.3
	vel	-136.7	99.9	0.1	0.5	-51.9	51.5	0.2	-0.8	-103.4	112.0	-0.8	1.0	-172.8	135.7	1.1	-0.8	-95.2	40.9	0.3	1.4	-80.3	41.4	0.9	1.5	-184.7	87.6	1.6	3.7
	accel	-949.7	924.4	-0.2	-3.1	-426.1	403.3	-0.8	3.7	-767.0	773.3	-9.6	-9.3	-1266.1	1214.3	12.1	-1.4	-868.7	868.2	-1.1	0.0	-512.4	602.1	3.5	-2.4	-1288.0	1494.7	7.3	0.0
	torTot	-216.9	9029.5	4717.1	4807.1	-432.3	2914.4	873.9	763.6	-896.8	1212.9	113.8	177.1	-1561.3	3073.1	1076.9	1449.0	-56.3	95.5	-1.1	2.2	-153.9	282.5	88.3	98.7	-5.4	39.4	4.8	3.0
	torAV	-6049.8	4172.2	25.3	26.1	-2533.3	1505.9	-21.5	12.1	-994.9	690.7	-16.2	4.6	-1440.7	1383.0	36.8	18.1	-62.2	84.5	1.8	0.6	-193.7	149.9	1.8	1.9	-15.2	21.0	0.4	0.0
act12	theta	16.7	31.3	24.9	25.5	41.3	84.0	65.4	65.8	-69.2	3.0	-31.6	-27.4	123.2	150.1	137.7	139.7	-16.4	14.3	-6.1	-8.8	-2.4	22.3	10.6	14.1	-124.6	-57.0	-94.4	-93.4
	vel	-17.9	16.2	-0.5	-1.0	-51.6	42.4	-1.4	0.6	-84.0	84.5	0.0	3.3	-35.5	35.0	-1.0	-1.0	-44.7	25.1	-1.1	-0.2	-34.0	24.5	-0.3	1.4	-76.9	59.8	-0.3	1.3
	accel	-136.0	134.6	-1.6	-3.9	-388.6	383.4	-0.2	-9.3	-640.7	672.8	-1.9	2.9	-253.1	245.5	5.7	0.6	-361.2	365.2	-2.2	0.8	-270.1	273.3	-1.9	6.5	-450.6	500.2	-5.8	1.9
	torTot	693.4	4490.7	2677.5	2852.9	964.0	2584.0	1885.2	2027.1	-505.8	763.1	125.7	228.9	-1439.2	1082.2	-139.5	-149.9	-35.1	43.7	8.2	7.8	-109.8	44.1	-27.9	-46.7	-23.1	-7.6	-16.7	-18.7
	torAV	-435.6	338.4	-0.6	-10.6	-687.9	646.9	3.4	-16.7	-367.7	258.8	-7.7	-7.4	-236.9	378.4	27.4	20.2	-8.3	3.7	-0.8	-0.5	-27.0	32.6	2.1	1.5	-2.4	5.6	0.2	0.0
act23	theta	19.3	49.8	35.8	41.3	87.0	123.9	104.7	98.9	-59.9	1.9	-22.3	-12.1	79.5	138.1	103.5	94.6	-32.2	55.2	9.2	-4.7	-60.1	-42.3	-51.8	-52.3	11.7	114.9	65.8	81.0
	vel	-32.5	35.4	1.0	1.1	-28.6	47.2	-0.7	-2.2	-62.9	70.6	0.0	0.3	-68.6	47.7	-0.5	-2.2	-127.2	95.9	-0.3	0.8	-42.5	29.6	0.6	-0.2	-106.4	141.7	0.1	-3.2
	accel	-263.2	278.4	0.5	0.8	-348.8	343.8	-1.4	-6.8	-550.8	533.7	2.6	-0.6	-464.5	495.4	-0.4	-1.7	-1011.9	963.6	2.0	4.4	-316.0	310.4	0.0	-5.3	-1103.3	1114.0	-1.2	-3.2
	torTot	-247.5	4883.8	2538.0	3447.3	128.9	3063.5	1282.8	788.4	1273.8	3100.8	1890.0	1931.3	-29.0	518.0	129.6	130.6	18.3	245.8	108.4	121.0	-14.6	39.6	1.8	-2.4	-20.8	18.2	-1.9	3.7
	torAV	-691.4	662.1	-2.7	3.4	-534.8	485.2	-17.9	-16.8	-710.0	704.3	-9.4	2.7	-173.2	216.3	4.9	2.8	-79.4	58.6	-2.0	-0.5	-15.4	21.4	-0.3	0.1	-4.6	6.3	0.2	0.2

These three actions represent three sub groups of actions including gross position actions (e.g. action 2), fine manipulation actions (e.g. action 8), and combined gross and fine manipulation (e.g. action 10). The results indicate that higher joint velocities of the shoulder and the elbow joints (axes 1-4) occur during gross positioning compared to lower velocities of the wrist joint (axes 5-7) – Fig. 4b. This relationship of velocity magnitudes between the two joint groups (axes 1-4 and axes 5-7) is inverted during fine manipulation. One may note that the velocity magnitudes of axes 5-7 during the fine manipulation tasks exceeded the velocity magnitudes of axes 1-4 during the gross positioning tasks. In the actions involving both gross positioning and fine manipulation, the maximal axis velocities were similar.

Fig. 4a (last row) depicts, for each joint, the total joint axis torque as well as the gravitational terms and the inertial, centrifugal, and Coriolis terms combined. In general, the magnitude of joint torque is small for the distal joint and higher for the proximal joints. Regardless of the joint location, the joint torque component that compensates the gravitational loads is significantly larger than the inertial, centrifugal, and Coriolis terms combined (Fig. 4a). In fact, the overall shape of the joint axis torque during the selected daily activities is dictated solely by the low frequency gravitational term.

Comparison of kinematics and dynamics of the human arm while eating with a spoon in a normal and emulated disabled spoon grasp indicates a significant increase of the shoulder joint range of motion and joint torque during the emulated disabled spoon grasp. These phenomena are also associated with lower magnitudes of shoulder joint axis velocities in the case of the emulated disabled spoon grasp (Fig. 6).

As a concluding result, Table I summarizes magnitude ranges of all kinematics and dynamic ranges along with mean and median values for actions 2, 8, 10, 12, and 23. Note the relative size between mean joint torques with and without gravitational components; total joint torques (torTot) are larger than the equivalent torques without gravity (torAV) by an order of magnitude or more. Comparing normal and power grasp methods of eating with a spoon, kinematic alterations are made to accommodate the abnormal grasp; severe pronation and ulnar deviation of the wrist leads to additional shoulder adduction and elbow extension.

IV. Conclusions and Discussion

Developing a powered exoskeleton that would serve a human operator adequately during daily activities requires a profound understanding of the kinematics and dynamics of the human arm during these activities, and is beyond the anthropometric information that has been widely known for several decades [2],[3]. The aim of this study was to study the kinematics and dynamics of the human arm and to provide the engineering specification to facilitate the design of a seven-degree of freedom powered exoskeleton.

The results indicate that the various joints' kinematics and dynamics change significantly based on the nature of the task. Gross position is usually achieved by utilizing the shoulder and the elbow joints with relatively low joint velocities. However, fine manipulations are performed by the wrist and forearm rotations with higher joint velocities. As expected, the joint torques decrease as we move from the proximal end of the arm to the distal end, which is also correlated with the muscular mass of the arm. Analyzing the contribution of individual terms of the arm's equations of motion indicate that the low frequency gravitational term is the most dominant term in these equations. The magnitudes of this term across the joints and the various actions is higher than the inertial, centrifugal, and Coriolis terms combined. These results justify using only the gravitational terms of the equations of motion as compensator in part of the control system.

Studying two different ways in which a human hand grasps an object (e.g. spoon or fork) indicates that although the operator's starting and ending points are the same and the tip paths are similar the arm joint kinematics and dynamics are different. The shoulder joint that is usually used for gross manipulation was utilized to compensate for the reduced flexion/extension of the wrist as well as the fine manipulation of the spoon by the fingers due to the power grasp. The shoulder joint compensations were pronounced by an increased range of motion as well as decreased velocity magnitudes. This result suggests that the exoskeleton might be utilized differently by a disabled person compared to a healthy operator due to specific and inherent disability regarding the range of motion of a specific joint or the method in which an object is grasped.

Acknowledgments

The authors wish to acknowledge the assistance provided by Dr. Glenn Klute and Michael Orendurff from the Veterans Affairs Puget Sound Health Care System - Center of Excellence for Limb Loss Prevention and Prosthetic Engineering in data collection using the VICON system. In addition, the authors wish to thank Jason Wan, Mike Rode, Mark Yamagishi, and John-Michael McNew for their help in data collection and post processing during a research project for graduate class (EE544) "Advanced Topics in Robotics".

References

[1] G.C. Burdea "Force and touch feedback for virtual reality", John Wiley & Sons Inc., 1996

[2] Military Handbook Anthropometry of US Military Personal, DOD-HDBK-747A, 1991

[3] Investigation of Internal Properties of the Human Body, DOT HS-801 430, 1975

[4] D.P. Romilly, C. Anglin,, R.G. Gosine, C. Hershler, S.U. Raschke, A functional task analysis and motion simulation for the development of a powered upper-limb orthosis, IEEE Transactions on Rehabilitation Engineering, vol. 2(3), pp. 119-129

[5] C.A. Stanger, C. Anglin, W.S. Harwin, D.P. Romilly, Devices for assisting manipulation: a summary of user task priorities, IEEE Transactions on Rehabilitation Engineering, vol. 2(4), Dec 1994. pp. 256 –265

[6] R. Ramanathan, S. Stroud, M.D. Alexander, "Powered Orthosis Project Forum," ASEL. Tech. Rep. TR #ROB9405. [Online]